Accepted version: doi: 10.1002/biot.201800545 ;

https://onlinelibrary.wiley.com/doi/abs/10.1002/biot.201800545

Towards Self-Regulated Bioprocessing: A Compact Benchtop Bioreactor System for Monitored and Controlled 3D Cell and Tissue Culture.

Sébastien de Bournonville[1,2,3]; Toon Lambrechts[1,4]; Johan Vanhulst[5]; Frank P. Luyten[1,6]; Ioannis Papantoniou[1,6*]; Liesbet Geris[1,2,3*]

[1]Prometheus, Division of Skeletal Tissue Engineering, KU Leuven, Leuven, Belgium

[2]Biomechanics Research Unit, U Liège, Liège, Belgium

[3]Biomechanics Section, KU Leuven, Leuven, Belgium

[4]M3- BIORES, KU Leuven, Leuven, Belgium

[5]Department of Materials Engineering, KU Leuven, Leuven, Belgium

[6]Skeletal Biology and Engineering Research Center, KU Leuven, Leuven, Belgium

* Shared senior authorship.

Correspondence: Mr. Sébastien de Bournonville, Mechanical engineering department, KU Leuven, Celestijnenlaan, B-3001 Heverlee, Belgium.

E-mail: sebastien.debournonville@kuleuven.be

Keywords: Bioreactor; Perfusion; Environment control; Tissue engineering; Biomanufacturing

Abbreviations: ATMP, advanced therapy medicinal product; **DO,** Dissolved oxygen; **GMP,** good manufacturing practice; **POC,** point of care; **hPDC,** human periosteum derived cell; **TE,** tissue engineering; **ID,** inner diameter; **OD,** outer diameter; **RH,** relative humidity.

Abstract

Bioreactors are crucial tools for the manufacturing of living cell based tissue engineered products. However, to reach the market successfully, higher degrees of automation as well as a decreased footprint still need to be reached. In this study, we assessed the use of a benchtop bioreactor for *in-vitro* perfusion culture of scaffold based TE constructs. A low footprint benchtop bioreactor system was designed, composed of single-use fluidic components and a bioreactor housing. The bioreactor was operated using an in-house developed program and the culture environment was monitored with specifically designed sensor ports. A gas exchange module was incorporated allowing for heat and mass transfers. Titanium based scaffolds were seeded with human periosteum derived cells and cultured for up to 3 weeks. The benchtop bioreactor constructs were compared to benchmark perfusion systems. Live/Dead stainings, DNA quantifications, glucose consumption and lactate production assays confirmed that the constructs cultured in the benchtop bioreactor grew similarly to the benchmark systems. Manual regulation of the system set-points enabled efficient alteration of the culture environment in terms of temperature, pH and dissolved oxygen. This study provides the necessary basis for the development of low-footprint, automated, benchtop perfusion bioreactors and enables the implementation of active environment control.

1 Introduction

The manufacturing of cell based advanced therapy medicinal products (ATMP) requires technologies that address both scaling and bioprocess challenges [1]. Bioreactors have been adopted as an enabling technology for ATMP production both for single cell as well as tissue culture [2; 3]. In contrast to static 2D culture in flasks or cell factories, bioreactors can incorporate sensors, allowing the identification and control of critical culture parameters such as temperature, pH, dissolved oxygen (DO) or the fluidic pattern (i.e. perfusion, mixing or agitation). This enables in-line or online monitoring of cells and their environment, all within a closed system. In addition, bioreactors have been advocated as cost efficient platforms, requiring less operator interventions to carry out ATMP manufacturing, while at the same time providing a low footprint solution for cell culture [4]. Indeed, the footprint is a major cost driver when these operations are carried out in GMP facilities.

Many dynamic bioreactor systems described in the literature consist of simple perfusion circuits in which a medium reservoir is linked to a culture vessel via a pump, and the whole circuit is placed inside an incubator for the control of environmental culture parameters [5; 6; 7; 8]. However, these approaches lack local environmental control and often the capability to host in-line sensors; this hampers robust production, automated operation as well as critical process parameter screening and monitoring. In addition, it does not allow for traceability and quality assurance of the final product. Recent efforts in the field have been made addressing these concerns, leading to a range of commercially available bioreactor systems, with environmental control features at different scales and different modes of operation. However, a high footprint and high cost of goods related to the use of these systems can impede their wide adoption and use. Table 1 shows a non-exhaustive but representative overview of existing bioreactor systems for stem cell therapies and tissue engineering (TE). The commercially available systems were collected based on the availability of technical specifications while some academic systems highlighting

environmental monitoring features were selected. All the systems were sorted per cell culture purpose and per level of environmental monitoring and control. From this table, one can observe the lack of in-line monitoring and environmental control features for TE applications.

In the context of patient-specific ATMP manufacturing (autologous approach), the use of sensor data-driven automated monitoring and control of the bioreactor becomes critical because of the inherent patient-related variability [10; 11; 12]. In that context, a need for change in manufacturing and delivery of stem cell ATMPs has been recognized [13]. Unlike an allogeneic process, in which every run theoretically starts with known, high-quality cells and predictable process behaviour, the starting material in an autologous process is highly variable, and might come from individuals with compromised health. The ideal bioreactor should therefore be able to monitor culture conditions and respond accordingly to assure that the resulting product has the appropriate critical quality attributes for every single patient [14]. Regarding the scale of operation, flexibility should be taken into account in the design of such a bioreactor to allow for adaptability to clinical indications and patient specific cell growth kinetics.

Altogether, the aforementioned arguments highlight the need for a standalone and automated bioreactor system with integrated sensors [14]. Such a system could be beneficial for the clinical translation of point of care (POC) treatments where the low footprint, automation and standalone capabilities are of significant importance. In this work, we present a closed bioreactor system whose footprint is significantly lower than most available systems. Using a non-standalone version of this fluidic (perfusion) set-up, we have previously reported on the expansion [15], harvest [16] and osteogenic differentiation of adult progenitor cells [17; 18]. As a proof of concept of the standalone system's capabilities, a scaffold-based perfusion culture of human periosteum derived stem cells (hPDCs) is reported here as a case study. The cells were cultured for up to 21 days in

the benchtop bioreactor, using automated media exchange while operating independently from an incubator (benchtop bioreactor system). We compared the outcome with perfusion rigs operating in incubators (benchmark systems). The objectives of this study were 1) to compare our benchtop system to the benchmark systems with a case study on the perfusion culture of human periosteum derived cells (hPDCs), 2) to monitor the culture environment and 3) to demonstrate its controllability.

2 Materials and methods

2.1 Bioreactor design

An incubator- independent unit was designed to gather all the hardware necessary for cell culture operations (cell seeding, expansion and tissue maturation) and environment control. This unit, further referred to as the bioreactor, was composed of three main parts: the bioreactor housing, the fluidic components and the connecting hardware for computer control. The frame of the system housing was 3D printed in polyamide and the windows were plexiglass. The tubing of the circuit was silicone, the feed-through connectors were polyoxomethylene and the perfusion chambers were machined out of polysulfon. The foot print of the resulting system was 0.0331m^3, approximately one log scale lower than most other systems (cf. Table 1). In this section, we describe the perfusion circuit and the three components making up the bioreactor, illustrated of Figure 1.

2.1.1 Perfusion circuit

Figure 1A illustrates a schematic of the bioreactor perfusion circuit. The system is operated by recirculating the medium from the medium reservoir (❶) to the perfusion chamber containing the TE construct (❺), while passing by a WMC series 150 peristaltic pump (❷, operating range: ~0.1 to 70 mL/min), a gas exchange module (❸) and a bubble trap device (❹), avoiding contact between the cells and air bubbles that could be trapped in the perfusion line. A sampling line (❻) allows medium removal by controlling pinch valve 3

(PV3). The circuit can be filled with fresh medium from an external reservoir (❼) using PV1.

By controlling PV 2, the medium can circulate in another loop bypassing the gas exchange module, the bubble trap and perfusion chamber. This bypass loop allows perfusing the circuit at high velocities when filling or sampling medium, while avoiding high shear stresses to the tissue construct in the perfusion chamber.

The perfusion chamber used in this system, for cell culture, can accommodate a cylindrical scaffold of around 2 cm in height, and a diameter of 6 mm. However, this bioreactor system can accommodate a novel design of perfusion chamber where larger or even multiple constructs can be cultured.

2.1.2 Bioreactor housing

The bioreactor housing encloses all the hardware necessary for the bioreactor operation. A picture of a prototype is shown in Figure 1G next to the computer that handles process control, data logging and visualisation. The bioreactor system within its housing is illustrated in Figure 1E. The housing encloses medium reservoir holders, the peristaltic pump, the three pinch valves, the gas exchange unit casing and the perfusion chamber holder. The fluidic components are assembled externally and fixed on these structures afterwards. An inlet for the controlled gas mixture was added in the housing to access the gas exchange module casing.

The bioreactor housing also includes all the necessary hardware for environment monitoring and control, namely: the heating elements, the thermometers and the electronic and optical connections that allow to bring sensors (O2, pH, temperature) close to the tissue construct.

Three temperature controllers were included in the housing for a) the reservoir and valves room (blue area on Figure 1A), b) the perfusion chamber room (red area on Figure 1A) and c) the gas exchange unit (❸ on Figure 1A).

2.1.3 Fluidic components

The fluidic components of the systems consist mainly of silicon tubing and Luer connectors linking the different elements of the perfusion circuit (cfr Section 2.1.1). A picture of the fluidic components of the main recirculating loop is shown on Figure 1F. Different tubing sizes were used in the different parts of the circuit. In general, thick tubing (Internal Diameter (ID) 1.6mm, Outer Diameter (OD) 4.8mm) was preferred in most parts of the tubing to limit water evaporation through the silicon membrane. Standard tubing (ID 1.6mm, OD 3.2mm) was used in the pinch valve parts and the peristaltic pump. Small tubing (ID 0.8mm, OD 2.4mm) was used in the gas exchange module to enhance mass and heat transfers (increased residence time and exchange surface area) while limiting the increase of medium volume in the circuit.

Luer connectors were used to make connections between the tubing and the reservoirs, the bubble trap and the perfusion chamber. Specific lids were manufactured for the recirculation to the medium reservoir while ensuring closing of the system.

It was observed that fluid pressure can increase at different locations of the circuit due to the numerous connections, junctions and angles in the circuit which could lead to leakages. Therefore, pressure release points were set at the reservoirs, using Millex®GP filter units to ensure sterility. The whole single-use fluidic circuits were gas sterilised each time before use.

2.1.4 Computer control

An in-house developed software code was implemented in MS Visual Studio for the bioreactor control and the gas mixer control. Figure 1A shows the bioreactor control software interface and Figures 1B-C-D show the gas mixer interfaces. The software allows the operator to manually control the various temperature set-points, the perfusion flowrate, the gas mixture and the gas flowrate.

In order to optimize the footprint of the system, a connecting metal rack was designed on which the bioreactor housing could be slid to allow for connection and control via the computer. This enabled easy handling of the system whilst maintaining flexibility for the user to disconnect the housing and bring it inside a sterile flow cabinet for operations on the biological construct.

2.2 Environment monitoring and control

2.2.1 Sensing

Specific sensor ports were designed at the inlet and outlet of the perfusion chamber. These ports enabled contact between the tip of a sensor and the culture medium, while ensuring dry sealing of the system and sterility. These sensor tips are depicted on Figures 1H-K. These sensor ports were designed to be able to host an optical fiber or electrical cable in order to carry different types of signal (Figure 1K).

A 4600 Model Thermometer (Measurement Specialties®) was adapted at the inlet of the perfusion chamber to provide continuous monitoring of the temperature of the medium going to the cells. Over the culture period, the temperature set-points of the bioreactor were manually regulated to maintain an optimal medium temperature around 37°C.

A SPOT (PreSens®) sensor was placed at the inlet of the perfusion chamber to monitor the pH of the medium. To demonstrate the ability to externally manipulate the culture environment, the pH was monitored for a perfusion flow rate of 1mL/min and a medium temperature stabilized at 37°C, while varying the concentration of CO2 in the gas mixture from 0% to 30% in steps of 5% (see Figure 2A for result). Such sensor port connections can also host dO2 sensor (PreSens®, OceanOptics®) or pCO2 sensors (PreSens®).

2.2.2 Evaporation

Evaporation of water out of the culture medium increases the salt concentrations and can be detrimental to the cultured constructs. Evaporation rates over the circuit were expected to be the highest in the gas exchange module since it was designed to enhance mass and

heat transfer. Therefore, a gas humidifier tank was designed to provide a high humidity environment in the gas exchange module casing. This allowed saturating the air surrounding the coil tubing and reducing evaporation out of the medium. Since the operation at a high relative humidity is restricted to the gas exchange module, the other bioreactor compartments can more easily house any other electronic components.

To verify the efficiency of the humidifier, the evaporation rate of the medium was quantified by measuring the change in metabolite concentrations over one week of perfusion without cells. Knowing the baseline metabolite concentrations, the change in concentration can be correlated to a volume change over time. The lactate and glucose concentrations were measured with a medium analyzer (Cedex Bio Analyzer®, Roche®) on the bioreactor with and without humidifier, and compared to benchmark perfusion circuits [19] [15] [20], running inside a 20% relative humidity (RH) incubator (see Figure 2D for results).

2.3 Bioreactor evaluation and construct growth assessment

In order to demonstrate the use of the bioreactor presented in this study as an in-vitro culture system for TE constructs, a case study on the perfusion culture of primary cell seeded scaffolds was performed.

2.3.1 TE constructs

Selective laser melted porous cylindrical Ti6Al4V scaffolds (OD 6mm and 6mm high) were used as carriers for the TE construct. The production and design details for these scaffolds were previously described [21]. In order to assure comparability of the results between the two culture setups, a controllable cell carrier was preferred over a potentially more biologically relevant carrier. Human PDCs [22], for which approval has been granted by the Ethical Committee of the University Hospital Leuven (ML7861_S53717), were drop seeded on the scaffolds (200 000 cells/scaffold) as previously described [15].

The constructs were cultured in both systems for up to three weeks at a perfusion flow rate of 0.1 mL/min, and the culture medium refreshed every 2-3 days.

2.3.2 Metabolite levels

Regular sampling of the culture medium was performed for each culture vessel and glucose and lactate metabolite concentrations were measured. Cumulative glucose consumption and lactate production profiles were calculated as an indicator of the cell growth dynamics. Evaporation of water from the culture medium was accounted for when calculating the production and consumption rates.

2.3.3 Live/Dead staining and DNA measurements

At the end of the culture period, a live/dead viability/cytotoxicity kit (Invitrogen®) was used to qualitatively evaluate cell viability in the constructs by fluorescent microscopy. The live/dead staining protocol was performed as previously described [15]. After imaging, constructs were prepared for DNA quantification using a quantitative and selective DNA assay (Quant-iTTM dsDNA HS kit, Invitrogen®). Constructs were rinsed in phosphate-buffered saline and the cells lysed in 350µL RLT lysis buffer (with 3.5µL β-mercaptoethanol, Qiagen). DNA was then quantified as previously described [23].

2.3.4 Quantitative PCR

For all samples, RNA was extracted and quantified using the RNeasy Mini Kit (Qiagen) and a Nanodrop ND-1000 spectrophotometer (Thermo Scientific), respectively. A RevertAid H Minus First Strand complementary DNA synthesis kit (Fermentas) was used for synthesis of complementary DNA and a Sybr green quantitative polymerase chain reaction was performed for different osteogenic and chondrogenic markers (Sox9, RunX2, Col1, ALP) and compared to HPRT (HPRT-F, 5'-TGAGGATTTGGAAAGGGTGT-3'; HPRTR, 5'-GAGCACACAGAGGGCTACAA-3'). The PCR reaction was cycled in a StepOnePlus™ PCR System (Thermo Fisher), as follows: 95°C for 10min, 40 cycles of 95°C for 15 s and 60°C for 60 s. Differences in gene expression were determined relatively in comparison to HPRT and shown as $2^{-\Delta CT}$.

2.3.5 Statistical analysis

An f-test analysis of variance followed by a t-test were performed to quantify significant differences in gene expression between the two groups, using Microsoft Excel (p=0.05 was considered significant).

3 Results

3.1 Monitoring and controllability of the environment

An important aspect of the bioreactor system developed in this study, was the environment control that houses the fluidic components. Its functionality ensures that the fluidic module is exposed to a controlled environment able to maintain stable conditions or change according to user demands. Sensor readings are shown on Figure 2A-C which highlights the monitoring capacity and controllability of the environment. Manual regulation of the temperature set-points allowed the medium at the inlet of the chamber to be kept close to 37°C (Figure 2C). From the pH readings, the system showed a response time in the range of 1 hour for a perfusion flowrate of 1mL/min. Figure 2A indicates of the sensitivity of the system to the applied CO2 concentration, enabled by the gas exchange module of the system. While so far the system displays relevant read outs to the operators for manual regulation of critical process parameters, no active control was done. However, all the necessary software and hardware is now set for implementation of active environment regulation.

The evaporation measurements on Figure 2D show the importance of the humidifier to limit evaporation in the process. The evaporation rate was decreased by 75% using the humidifier and reached values comparable to the simple systems, running inside incubators.

3.2 Validation case study

Cell presence and activity within the fluidic circuit was verified and measured using a number of assays over time. The results of the Live/Dead staining are shown on Figures 2E-J. This figure highlights the living cells (green dye) colonizing the inner space of the scaffold after three weeks of culture. In both systems, for each run, very small amounts of dead cells

(red dye) were observed. The cumulative lactate production and glucose consumption profiles of the constructs are shown on Figures 2K-L. These were calculated relatively to day 0 of culture (seeding day), when no lactate or glucose had been produced or consumed, respectively. The DNA content of the constructs at week 3 in the benchtop bioreactor reached 8.05±2.21µg of DNA (N=3) while constructs cultured in the benchmark systems reached an amount of 7.00±2.80µg of DNA (N=7) (Figure 2M).

3.3 Gene expression analysis

The results of the relative gene expression levels are shown on Figure 2N-Q. The analyses revealed no significant differences in the expressions of Sox9 (2.7±0.4 and 2.5±0.5 fold increase compared to housekeeping gene) and ALP (0.7±0.4 and 0.9±0.2 fold increase) between the benchtop and the benchmark systems, respectively. Col1 (573.5±67 and 425.8±90.6 fold increase) and RunX2 (3.4±0.8 and 2.3±0.5 fold increase, respectively) were significantly upregulated in the benchtop bioreactor compared to the benchmark system.

4 Discussion & concluding remarks

Bioreactors are a valuable tool for bringing TE products to the market [24]. However, there are a certain number of design elements that are required for a successful clinical translation [25; 26]. These include (I) a closed loop system to assure sterility, (II) use of biocompatible materials, (III) precise monitoring and control of the 3D cellular environment, (IV) and integration in GMP production facilities both from a practical and a regulatory perspective. Additionally, to assure the economic viability of the bioreactor it has to be able to serve multiple cell therapy and TE applications, which in turn requires a certain degree of modularity.

The bioreactor design described in this study consists of a housing hosting a closed loop perfusion circuit. This arrangement ensures no contact between culture medium and external environment, limiting the risk of contamination. Additionally, a slight overpressure is created in the housing via the outlet of the gas exchange module, preventing external

contaminants from entering the system. Whilst during the initial setup of the bioreactor system it is still required to make sterile connections in a biosafety cabinet, medium refreshment and sampling during normal operations can be done automatically via the bioreactor's user interface.

The materials used for the perfusion system were selected for biocompatibility and screening experiments were performed in which cells were exposed to media conditioned with the materials used to verify that there was no cytotoxicity. The data presented here show that the bioreactor supports long-term growth (up to 3 weeks) of adult progenitor cells (MSC-like) cells. Indeed, experimental results presented in Section 3.2 indicate that the cells seeded in the scaffolds and cultured over 3 weeks could proliferate and colonize the scaffolds similar to the benchtop bioreactor and the benchmark system (cfr Figures 2 E-M). In both bioreactors, hardly any dead cells were observed at the end of the culture indicating a viable cell population. Cells were able to bridge pores and grow in 3rd dimension as has been demonstrated through the use of microCT analysis in previous studies [19]. Metabolite measurements showed cumulative lactate production and glucose consumption curves of proliferating constructs (Figures 4K-L), with no significant differences between both vessels. Quantification of DNA (Figure 4M) indicated similar cell yields between the two operating conditions.

In the context of adult mesenchymal stromal cell types the transcription factors investigated here can be correlated to the presence of osteo- (RunX2 [27]) and chondro- (Sox9 [28]) progenitor cell subpopulations and their subsequent respective lineage commitment and differentiation trajectories. In addition Col1 gene expression is an indicator of early osteogenesis [29]. There was no difference observed in Sox9 expression while RunX2 was upregulated in the benchtop bioreactor system. This could suggest a slight commitment to osteoprogenitor cells also supported by the statistically significant (although small) upregulation of Col1. However it does not suggest osteogenic differentiation since ALP, a

later differentiation marker [30], was slightly downregulated. These small gene expression differences could be also explained by technical differences across the two systems. For example the flow profile developed due to different pumps would affect the frequency of pulsatile flow to which the cells were exposed and hence could affect mechanosensitive genes, such as the ones analyzed here ([29; 31]). Taken together, these data illustrate that the bioreactor system was capable of supporting scaffold-based 3D progenitor cell cultures.

The bioreactor housing is equipped with multiple (optical) sensor connections and a custom developed sensor connection was designed, able to bring lab-scale sterilisable in-line sensors as close as possible to the TE construct in order to monitor and control the microenvironment of the construct. Additionally, the bioreactor has an integrated incubator system, which facilitates environmental regulation dynamics (heat and mass transfer) and therefore increases the environmental control precision but also opens up new possibilities for model-based control, scalability and increased robustness [32].

Apart from the environmental control, a custom-made program was developed to visualise the state of the system, encompassing the environmental parameters and sensor readings as well as the position of the valves and the remaining volume in the medium reservoir. In addition, the software centralises these readouts from multiple bioreactor systems running in parallel. This enables data traceability of the environment and process parameters, as required for GMP production.

The integrated incubator in the bioreactor also allows for a smaller footprint of the system, evaluated to a log scale smaller than available systems. Footprint minimization is important for the integration of the system in manufacturing facilities where space (and especially incubator space) is a main cost consideration. Moreover, the high humidity environment of incubators impedes the implementation of advanced sensor systems and electronic components in the bioreactor housing. The lack of sensor integration in turn makes product characterisation and comparability of the product (e.g. between multiple production sites)

and – by extension – the integration of the bioreactor system in a GMP production environment more challenging. Additionally, the bioreactor housing with three valves, integrated incubator, multiple sensor connections, a versatile environmental control and easily controllable peristaltic pump can be equipped with different layouts of the fluidic systems with differently designed (perfusion) chambers and therefore multiple TE applications can be targeted.

The use of monitored and controlled bioreactors allows process automation (e.g. automated liquid transfer steps). Together, these steps serve not only to reduce the cost for patient-specific manufacturing but also to enhance process robustness. In addition, the low footprint could allow scale-out strategies whereby multiple batches are simultaneously manufactured, potentially in multiple non-centralized facilities. In the case of individualized bioprocessing, the production could often aim to take place close to the bedside of the patient (distributed manufacturing). These versatile and low footprint compact devices could also be adopted for POC manufacturing within hospital facilities, which could be an alternative strategy for manufacturing autologous MSC-based ATMPs, in contrast to a more centralized manufacturing model [4].

In this work, a novel bioreactor system was presented, having the ability to provide solutions for automated cell therapy bioprocessing. Such automated, low footprint, closed systems could support operation outside of clean room environments while minimising human intervention and therefore providing a cost-effective and less variable alternative to existing systems. By validating this new culture set up, we demonstrated the feasibility of TE construct culture in a benchtop and incubator-independent environment. The culture environment provided by this new system could be monitored and effectively regulated thanks to the sensors and the operation software. These results go one step further in the development of more robust systems as the manual labour associated to the handling of these culture vessels was strongly reduced.

Acknowledgement

S.d.B. was supported by a PhD grant of the Research Foundation Flanders (FWO, Grant No. 1S67217N, www.fwo.be). T.L. was supported by a postdoctoral grant of the Flemish Agency for Innovation and Entrepreneurship (VLAIO). F.L. acknowledges support by the European Research Council under the European Union's Seventh Framework Programme (Grant No. FP7/2007-2013/ERC, 249191). I.P. was funded by a Research Foundation of Flanders fellowship (FWO project number: 12O7916N). L.G. acknowledges support by the European Research Council under the European Union's Seventh Framework Programme (Grant No. FP7/2007-2013/ERC, 279100 and H2020/2013-2020/ERC, 772418). This study was part of Prometheus, the Leuven Research and Development Division of Skeletal Tissue Engineering of KU Leuven: www.kuleuven.be/prometheus

Conflict of interest

The authors declare no financial or commercial conflict of interest.

5 References

[1] Lambrechts, T., Sonnaert, M., Schrooten, J., Luyten, F., et al., Large-Scale Mesenchymal Stem/Stromal Cell Expansion: A Visualization Tool for Bioprocess Comparison. Tissue Eng Part B Rev. 2016, 22, 485-498.

[2] Nokhbatolfoghahaei, H., Rad, M., Khani, M., Shahriari, S., et al., Application of Bioreactors to Improve Functionality of Bone Tissue Engineering Constructs: A Systematic Review. Curr Stem Cell Res Ther. 2017, 12, 564-599.

[3] Mitra, D., Whitehead, J., Yasui, O., Leach, J., Bioreactor culture duration of engineered constructs influences bone formation by mesenchymal stem cells. Biomaterials. 2017, 146, 29-39.

[4] Abraham, E., Ahmadian, B., Holderness, K., Levinson, Y., McAfee, E., Platforms for Manufacturing Allogeneic, Autologous and iPSC Cell Therapy Products: An Industry Perspective. Adv Biochem Eng Biotechnol. 2017, DOI: 10.1007/10_2017_14.

[5] Grayson, W., Bhumiratana, S., Cannizzaro, C., Chao, P., et al., G. Effects of initial seeding density and fluid perfusion rate on formation of tissue-engineered bone. Tissue Eng Part A. 2008, 14, 1809-1820.

[6] Talò, G., Turrisi, C., Arrigoni, C., Recordati, C., et al., Industrialization of a perfusion bioreactor: prime example of a non-straightforward process. J Tissue Eng Regen Med. 2018, 12, 405-415.

[7] Bhumiratana, S., Bernhard, J., Alfi, D., Yeager, K., et al., Tissue-engineered autologous grafts for facial bone reconstruction. Sci Transl Med. 2016, 8, 343ra83.

[8] Volkmer, E., Drosse, I., Otto, S., Stangelmayer, A., et al., Hypoxia in static and dynamic 3D culture systems for tissue engineering of bone. Tissue Eng Part A. 2008, 14, 1331-1340.

[9] Schuerlein, S., Schwarz, T., Krziminski, S., Gätzner, S., et al., A versatile modular bioreactor platform for Tissue Engineering. Biotechnol J. 2017, 12, DOI: 10.1002/biot.201600326.

[10] Lambrechts, T., Papantoniou, I., Rice, B., Schrooten, J., Luyten, F., Aerts, J., Large-scale progenitor cell expansion for multiple donors in a monitored hollow fibre bioreactor. Cytotherapy. 2016, 18, 1219-1233.

[11] Heathman, T., Rafiq, Q., Chan, A., Coopman, K., et al., Characterisation of human mesenchymal stem cells from multiple donors and the implications for large scale bioprocess development. Biochemical Engineering Journal. 2016, 108, 14-23.

[12] Papantoniou, I., Lambrechts, T., Aerts, J., Bioprocess engineering strategies for autologous human MSC-based therapies: one size does not fit all. Cell Gene Therapy Insights. 2017, 3, 469-482.

[13] Trainor, N., Pietak, A., Smith, T., Rethinking clinical delivery of adult stem cell therapies. Nat Biotechnol. 2014, 32, 729-735.

[14] Levinson, Y., Beri, R., Holderness, K., Ben-Nun, I., et al., Bespoke cell therapy manufacturing platforms. Biochemical Engineering Journal. 2018, 132, 262-269.

[15] Sonnaert, M., Papantoniou, I., Bloemen, V., Kerckhofs, G., et al., Human periosteal-derived cell expansion in a perfusion bioreactor system: proliferation, differentiation and extracellular matrix formation. Journal of tissue engineering and regenerative medicine. 2017, 11, 519-530.

[16] Sonnaert, M., Luyten, F., Schrooten, J., Papantoniou, I., Bioreactor-Based Online Recovery of Human Progenitor Cells with Uncompromised Regenerative Potential: A Bone Tissue Engineering Perspective. PLoS One. 2015, 10, DOI: 10.1371/journal.pone.0136875.

[17] Papantoniou, I., Sonnaert, M., Lambrechts, T., Aerts, J., et al., Analysis of Gene Expression Signatures for Osteogenic 3D Perfusion-Bioreactor Cell Cultures Based on a Multifactorial DoE Approach. Processes. 2014, 2, 639-657.

445 [18] Papantoniou, I., Chai, Y., Luyten, F., Schrooten, J., Process quality engineering for
446 bioreactor-driven manufacturing of tissue-engineered constructs for bone regeneration.
447 Tissue Eng Part C Methods. 2013, 19, 596-609.
448 [19] Papantoniou, I., Sonnaert, M., Geris, L., Luyten, F., et al., Three-dimensional
449 characterization of tissue-engineered constructs by contrast-enhanced nanofocus
450 computed tomography. Tissue Eng Part C Methods. 2014, 20, 177-187.
451 [20] Zhou, X., Holsbeeks, I., Impens, S., Sonnaert, M., et al., Noninvasive real-time monitoring
452 by alamarBlue(®) during in vitro culture of three-dimensional tissue-engineered bone
453 constructs. Tissue Eng Part C Methods. 2013, 19, 720-729.
454 [21] Van Bael, S., Kerckhofs, G., Moesen, M., Pyka, G., et al., Micro-CT-based improvement of
455 geometrical and mechanical controllability of selective laser melted Ti6Al4V porous
456 structures. Mat Sci Eng a-Struct. 2011, 528, 7423-7431.
457 [22] De Bari, C., Dell'Accio, F., Vanlauwe, J., Eyckmans, J., et al., Mesenchymal multipotency
458 of adult human periosteal cells demonstrated by single-cell lineage analysis. Arthritis
459 Rheum. 2006, 54, 1209–1221.
460 [23] Chen, Y., Sonnaert, M., Roberts, S., Luyten, F., Schrooten, J., Validation of a PicoGreen-
461 based DNA quantification integrated in an RNA extraction method for two-dimensional and
462 three-dimensional cell cultures. Tissue Eng Part C Methods. 2012, 18, 444-452.
463 [24] Martin, I., Wendt, D., Herberer, M., The role of bioreactors in tissue engineering. Trends
464 Biotechnol. 2004, 22, 80-86.
465 [25] Martin, I., Smith, T., Wendt, D., Bioreactor-based roadmap for the translation of tissue
466 engineering strategies into clinical products. Trends Biotechnol. 2009, 27, 495-502.
467 [26] Plunkett, N., O'Brien, F., IV.3. Bioreactors in tissue engineering. Stud Health Technol
468 Inform. 2010, 152, 214-230.
469 [27] Wei, J., Shimazu, J., Makinistoglu, M.P., Maurizi, A., et al., Glucose Uptake and Runx2
470 Synergize to Orchestrate Osteoblast Differentiation and Bone Formation. Cell, 2015, 161(7),
471 1576-1591.
472 [28] Akiyama, H., Chaboissier, M.C., Martin, J.F., Schedl, A., de Crombrugghe, B., The
473 transcription factor Sox9 has essential roles in successive steps of the chondrocyte
474 differentiation pathway and is required for expression of Sox5 and Sox6. Genes Dev., 2002,
475 16(21), 2813-2828.
476 [29] Brindley, D., Moorthy, K., Lee, J.H., Mason, C., et al., Bioprocess Forces and Their Impact
477 on Cell Behavior: Implications for Bone Regeneration Therapy. J Tissue Eng., 2011, 620247
478 [30] Aubin, J.E., Regulation of osteoblast formation and function. Rev Endocr Metab Disord.,
479 2001, 2(1), 81-94.
480 [31] Kim, K.M., Choi, Y.J., Hwang, J.H., Kim, A.R., et al., Shear stress induced by an interstitial
481 level of slow flow increases the osteogenic differentiation of mesenchymal stem cells
482 through TAZ activation. PLoS One., 2014, 9(3), e92427.
483 [32] Lambrechts, T., Papantoniou, I., Sonnaert, M., Schrooten, J., Aerts, J.M., Model-based cell
484 number quantification using online single-oxygen sensor data for tissue engineering
485 perfusion bioreactors. Biotechnol Bioeng. 2014, 111, 1982-1992.
486

Table 1. Commercially available bioreactors and reported culture systems in literature for stem cell therapies and tissue engineering. *The footprint was estimated here from the space occupied by all the hardware necessary for culture operation, from manufacturer data, including circuitry (tubing, pump, gas exchangers, bubble trap, cell culture module), sensors, computers, gas mixer and incubators. The systems annotated with †. require an external incubator for operation, thus the footprint of a standard incubator was estimated (Steri-Cult®, Thermo Scientific). **Suitability for Point of Care evaluates the ease of integration of the culture system in a decentralized manufacturing approach (bedside). N.a.: information not available; susp.: suspension.

Authors or manufacturers	**Environmental control**	**Footprint***	**Suitable for point of care** (POC)**	**Cell culture mode and purpose**
Octane Cocoon™	Interated pH and dO2 monitoring. Bioresponse feedback	~0.3m^3	Potential solution	• Cell Expansion & Tissue development • Suspension, planar and Scaffold/fixed-bed
Scinus Cell Expansion™	Integrated pH, dO2 and biomass monitoring.	~0.4m^3	No	• Cell expansion • Suspension
VivaBioCell NANT 001	No integrated sensor. Circuit incubation, pH estimation	~0.24m^3	No	• Cell expansion • Planar
Quantum® Terumo BCT	No integrated sensors. Circuit incubation	~0.5m^3	No	• Cell expansion • Hollow fibre
Xpansion® Pall	Yes	~0.5m^3 (inc.)	No	• Cell expansion • Planar

Xuri™ Cell expansion	Yes	~0.4m^3	No	• Cell expansion • Suspension
3D Biotek perfusion bioreactor	No	~0.75m^3 (inc.)	No	• Cell expansion • Scaffold/fixed-bed
Pluristem 3D manufacturing platform	Yes	~0.72m^3	No	• Cell expansion • Scaffold/fixed-bed
Aglaris Facer 1.0™	Yes	~0.48m^3	No	• Cell expansion • Suspension
Grayson et al. (1)	No	~0.75m^3 (inc.)	No	• Tissue development • Scaffold/fixed-bed
Talò et al. (2)	No	~0.75m^3 (inc.)	No	• Tissue development • Scaffold/fixed-bed
Schuerlein et al. (3)	Yes	~0.09m^3	Potential solution	• Tissue development • Scaffold/fixed-bed
Bhumiratana (4)	No	~0.75m^3 (inc.)	No	• Tissue development • Scaffold/fixed-bed
Volkmer et al. (5)	No	~0.75m^3 (inc.)	No	• Tissue development • Scaffold/fixed-bed

Figure legends

Figure 1. Presentation of the benchtop bioreactor designed in this study. **A**: Software interface for bioreactor control. A scheme of the circuit is drawn (bubble trap ❹ not included, see **F**), showing the readings of the several temperature sensors and allowing to control the perfusion flowrate, the states of the valves and the temperature set-points. Pre-implemented functions allow removing or filling a specific amount of medium with functional buttons. **B**: Software interface of the gas mixer, allowing controlling the mixture of the gas going to the gas-exchange module and the flowrate. **C**: Real-time graph of the measured gas flow rates (N2, O2 and CO2) at the output of the gas mixer. **D**: Real-time graph of the chosen set-points of the gas mixture. **E**: Illustration of the bioreactor housing. **F**: Picture of a prototype of the bioreactor, highlighting the fluidic components of the recirculation loop and the internal configuration of the oxygenator. **G**: Benchtop setup. A prototype of the bioreactor is shown on the right, next to the computer. **H**: Perfusion chamber designed for this study (shown upside down). The white sensor ports are shown.

511 The blue light (pointed by the yellow arrow) shows the tip of the pH sensor at the inlet of
512 the chamber. Six sensor ports are available for monitoring at the inlet and the outlet (3 each,
513 see front view ❺ on **A**) of the perfusion chamber. **I-J**: Schematic cuts highlighting how
514 contact is made between the tip of the sensor ports while maintaining the closure of the
515 circuit. The red vector shows the perfusion direction. **K**: Schematic cut of a sensor port, the
516 different coloured patches show how different sensor types (thermos-resistor, pH, dO2 of
517 pCO2 sensitive patches) can be adapted.
518 **Figure 2.** Comparison of in-vitro culture results and environment modulation results. **A**: pH
519 value at the steady state (taken from **B** after the signal stabilized) as a function of the applied
520 CO2 concentrations. **B**: Time series of the pH readings at the inlet of the perfusion chamber
521 (medium perfused at 1mL/min). The blue and green line respectively show the raw
522 readings and the Gaussian filtered readings from the sensor (left y-axis). The orange line
523 shows the time series of the applied CO2 concentrations (right y-axis). **C**: Temperature
524 sensor readings at the inlet of the perfusion chamber over a construct culture of 21 days.
525 The red dash-dotted line shows the optimal objective temperature of 37°C. The sensor
526 signal was filtered with a Gaussian filter to eliminate artefacts due to regular disconnections
527 of the bioreactor prototype for medium refreshments. **D**: Evaporation rates calculated from
528 metabolites measurements on the basic circuits set inside incubators (white bar), the NBR
529 with the humidifier tank (black bar) and without (gray bar). **E-J**: Live/Dead staining results
530 on TE constructs cultured in the new bioreactor (**E-G**) and in the basic perfusion circuits (**H-**
531 **J**) after 3 weeks at 0.1 mL/min flow rate. The green dye stains the living cells while the red
532 dye stains the nuclei of the dead cells (scale bars: 1mm, the constructs are 6x6x6 mm). The
533 red vectors show the direction of the culture medium flow. Top (**E, H**), side (**F, I**) and bottom
534 (**G, J**) views of the samples are shown. **K-L**: Cumulative lactate production (mmol, **K**) and
535 glucose consumption (mmol, **L**) of the constructs over the culture time. The empty marker
536 show average cumulative values for the basic perfusion circuits (N=10), with standard

deviations (black bars). **M**: DNA content of constructs cultured for 3 weeks at 0.1 mL/min in the new bioreactor (black, N=3) and in the basic perfusion circuits (white, N=7), error bars. **N-Q:** relative mRNA expression levels of Sox9 (**N**), RunX2 (**O**), Col1 (**P**) and ALP (**Q**) compared to the housekeeping gene (HPRT). The error bars show the standard deviation and an asterisk indicates a statistically significant difference ($p<0.05$).

Figures

Figure 1.

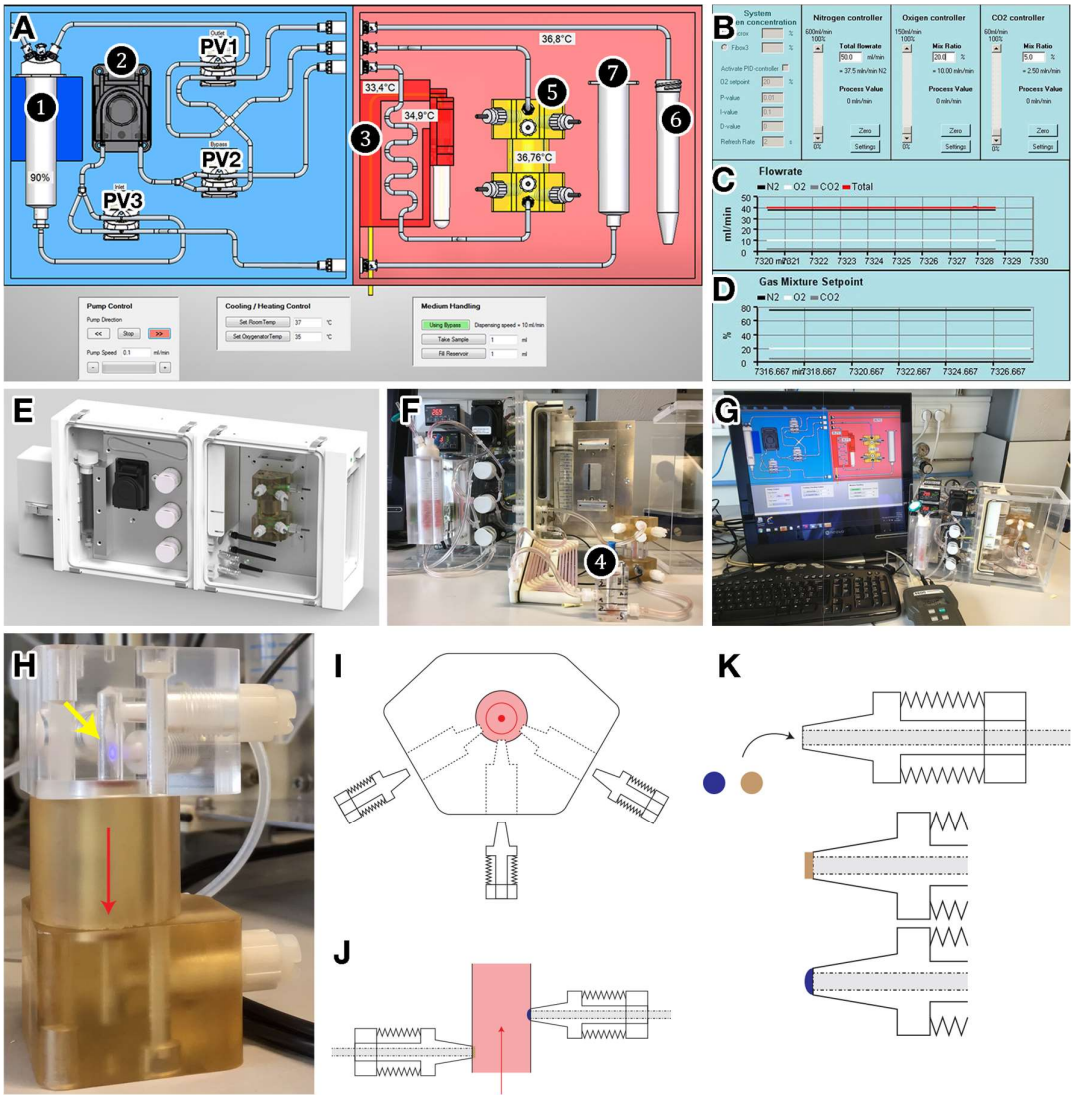

Figure 2.

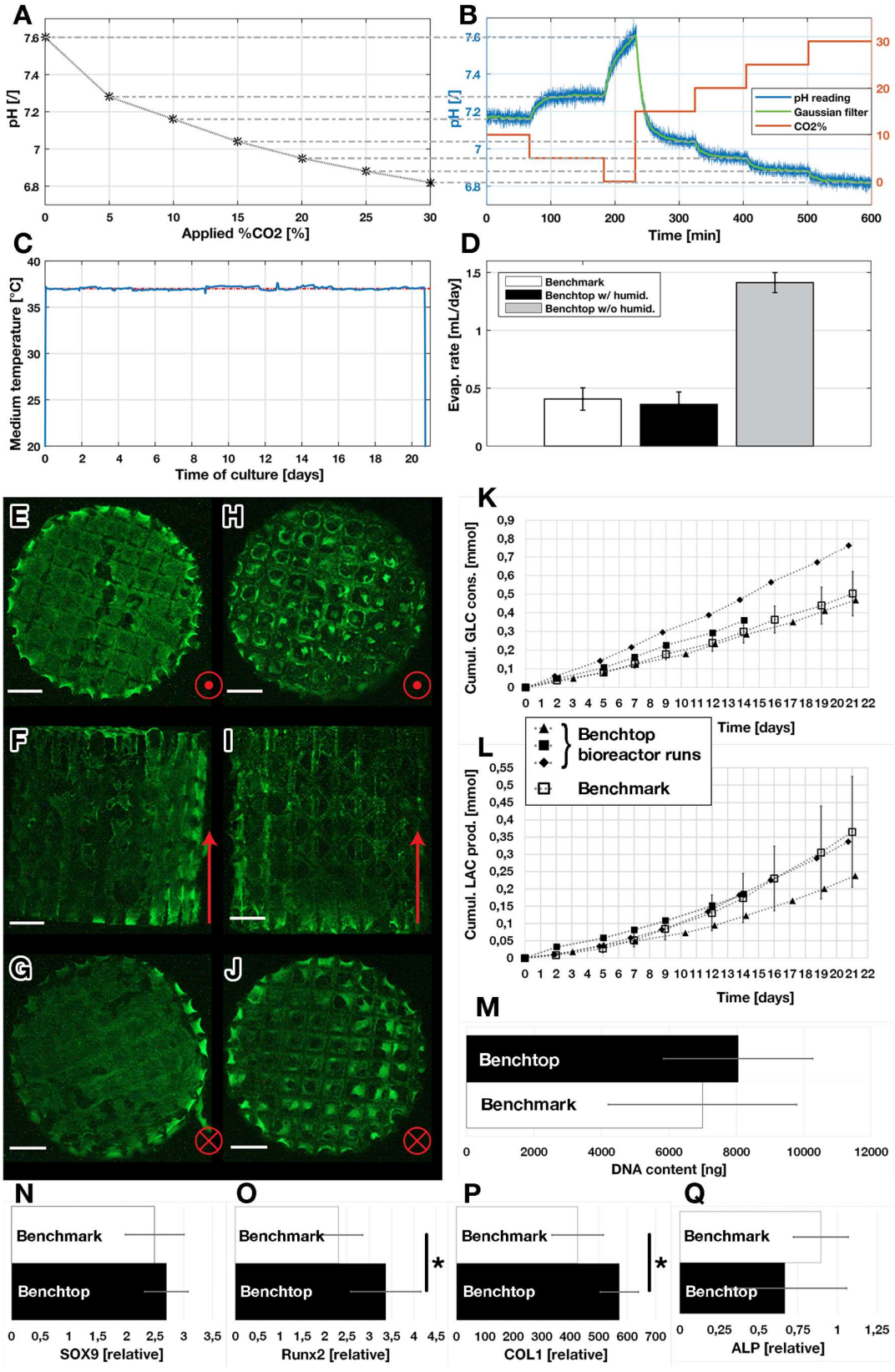
A
pH [/]
Applied %CO2 [%]
B
pH [/]
Time [min]
pH reading
Gaussian filter
CO2%
C
Medium temperature [°C]
Time of culture [days]
D
Evap. rate [mL/day]
Benchmark
Benchtop w/ humid.
Benchtop w/o humid.
E
H
F
I
G
J
K
Cumul. GLC cons. [mmol]
Time [days]
Benchtop bioreactor runs
Benchmark
L
Cumul. LAC prod. [mmol]
Time [days]
M
Benchtop
Benchmark
DNA content [ng]
N
Benchmark
Benchtop
SOX9 [relative]
O
Benchmark
Benchtop
Runx2 [relative]
P
Benchmark
Benchtop
COL1 [relative]
Q
Benchmark
Benchtop
ALP [relative]

547